Indian Journal of Chemistry
Vol. 62, December 2023, pp. 1298-1302
DOI: 10.56042/ijc.v62i12.5901

Electrocatalytic activity of Ni/Co_3O_4 obtained by span-60 sol-gel route for oxygen evolution in 1M KOH at 25°C

Basant Lal*, Brajesh Gangwar & Pankaj Chauhan

Department of Chemistry, Institute of Applied Sciences and Humanities, GLA University, Mathura 281 406, India
E-mail: basant.lal@gla.ac.in

Received 30 September 2023; accepted (revised) 24 November 2023

Spinel-type cobalt oxide (Co_3O_4) was prepared by the span-60 sol-gel (SSG) method by using cobalt nitrates and span-60 and characterized by FT-IR, XRD and SEM techniques and its catalytic performance for electrochemical formation of oxygen in a basic medium is investigated. For electrochemical studies, cyclic voltammetry and Tafel polarisation techniques were employed and the observed results of investigation showed that the Co_3O_4 electrode possessed higher value of oxide roughness factor and hence have improved electrocatalytic activity for the oxygen evolution process (OER) in basic solution. The Tafel slope at low over potential and order of reaction with regards to the variation of $[OH^{-}]$ concentration were found to be 73 $mVdec^{-1}$ and (~1), respectively. The thermodynamic parameters such as standard electrochemical activation energy estimated from the Arrhenius plot and entropy of reaction were 35 $kJmol^{-1}$ and 259 $Jdeg^{-1}mol^{-1}$ for the OER. Highly negative value of entropy of the reaction indicated that electrocatalytic oxygen evolution by splitting water occurs *via* the mechanism involving the adsorption of reaction intermediate at the electrode surface.

Keywords: Sol-gel combustion synthesis, Span-60, Tafel polarisation, OER, Cyclic voltammetry

In our daily lives, people consume energy in a variety of ways. The majority of it is produced by burning finite fossil fuels and is in the form of electrical energy. Since fossil fuel combustion releases significant amounts of carbon dioxide into the atmosphere, it is necessary to find different energy sources to reduce our reliance on fossil fuels. The demand for environmentally friendly and sustainable energy conversion, which encourages large-scale storage of wind and solar electricity into fuels, has reignited interest in electrochemical and photo-electrochemical water splitting[1]. The creation of commercially effective electrocatalyst materials for the oxygen evolution reaction is a significant obstacle in this field. These criteria have attracted a lot of interest to transition-metal oxide catalysts, spinel-type cobalt oxide nanoparticles (Co_3O_4NPs) are among them, and they have drawn a lot of interest because of their special properties and potential uses as gas sensors[2], heterogeneous catalysts[3], electrochemical devices[4], Li-ion batteries[5-6], magnetic materials[7], and photocatalysts[8-9]. Because particle size and morphology have an impact on the properties and uses of Co_3O_4 nanoparticles, there has been an increase in interest in their synthesis during the past few years[10-15]. These substances are readily available on Earth, need little preparation, and have good catalytic stability in both alkaline and neutral electrolytes[16-18]. Cobalt oxides can be made either amorphously or crystalline using several techniques, such as Thermal salt decomposition[19], Autoclave synthesis[20], Sol-gel synthesis[21], Co-electrode position and Subsequent oxidation[22], Direct oxide electrodeposition[23-25] and Photochemical reactions[16,26].

In the present investigation, an effort has been made to synthesize Co_3O_4 in economical way by low temperature sol-gel route using span-60 and cobalt(II)nitrate hexahydrateas precursors without using solvent, surfactant, and complicated equipment. The oxide was characterized by Fourier transforms infrared spectroscopy (FT-IR), X-ray diffraction (XRD), scanning electron microscopy (SEM), and electrochemical measurements for oxygen evolution reaction in basic medium.

Materials and Methods

Synthesis of Co_3O_4

All the reagents were of analytical grade and utilized without further purification. Cobalt(II)nitrate hexahydrate (ACS reagent≥98) was purchased from Sigma Aldrich (United Kingdom) and Span-60 was purchased from CDH (India). The preparation of

Co_3O_4 nanoparticles is achieved with desired amount of span-60. First of all, cobalt(II)nitrate hexahydrate was mixed in molten Span-60 with continuous stirring and further dried till the mixture transformed into a dark reddish gel form. Further, the resultant gel was calcined in PID controlled electrical muffle furnace at 350°C for 5 hrs to obtain spinel oxide.

Characterization techniques

FT-IR spectroscopy and XRD spectroscopy were used to establish the formation of a spinel-type oxide. The FT-IR spectrum of oxide was recorded from the wavenumber of 400 to 4000 cm^{-1} on the IRSPIRIT-T Shimadzu spectrophotometer and for XRD powder pattern, Cu-Kα- as the source of radiation, λ = 1.54059 Å and examined from the phase angle of 2θ = 20 to 80^o. Morphology and particle size were observed by scanning electron microscopy with the help of a Zeiss scanning electron microscope.

For the electrochemical study, the oxide electrode was fabricated by the repeated coatings of oxide slurry with triton X-100onto the one side pre-treated nickel plate in concentrated HCl, rinsed in acetone ultrasonically and washed with double distilled water, and subsequently sintered in an electrical furnace at 300°C for 1 hr to have oxide loading of ~ 5 mg cm^{-2}. For electrical contact, a flattened end of copper wire was connected with the opposite side of the nickel plate using silver paste and mounted with epoxy resin (Araldite) leaving an exposed oxide area (~0.5 cm^{-2})[27]. Electrocatalytic properties of the fabricated electrodes were performed in a single compartment pyrex glass cell that consists of three electrodes system having a working electrode (Ni/oxide electrode), a counter electrode (graphite rod) and a reference electrode (Hg/HgO/1MKOH (0.098V *vs* NHE)) using the CHI electrochemical work station.

Results and Discussion

FT-IR analysis

Fig 1 depicts the FT-IR spectrum of Co_3O_4 oxide nanoparticles with the Co^{2+}–O and Co^{3+}–O stretching vibrations of two prominent peaks in the IR spectra at 659 and 555 cm^{-1}, respectively[28]. These peaks are caused by the spinel structure of cobaltite nanoparticles, tetrahedral and octahedral sites. Due to adsorbed water molecules stretching and bending vibration, two faint peaks were identified at 3735 and 1636 cm^{-1}. Furthermore, a tiny peak at 2357 cm^{-1} is seen, indicating the presence of carbon dioxide.

XRD analysis

In specified phase angle regions ranging from 20 to 80 degrees, XRD powder pattern diffraction of synthesized oxide Co_3O_4 was performed and shown in Fig 2. XRD powder patterns showed the formation of the nano-size crystalline oxide structure with the corresponding peaks (220), (311), (400), (422), (511), and (440) XRD planes identical with those given in JCPDS file No. 76-1802. The value of crystallite size of cobaltite is estimated by the full width at half maximum (FWHM) of the most intense peak in XRD spectrum using the Debye Sherrer formula $\left(S\frac{0.9\times\lambda}{\beta\cos\theta}\right)$ where S is crystallite size, θ is Bragg angle. The calculated value of crystallite size of cobaltite is ~20 nm. For the spinel oxide prepared by the sol-gel auto combustion method using span–60, calculated values of crystallite size is

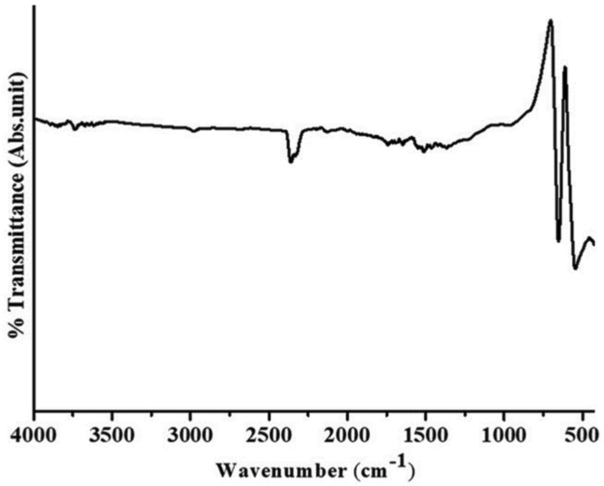

Fig 1 — FT-IR spectrum of Co_3O_4 prepared at 350°C for 5 h

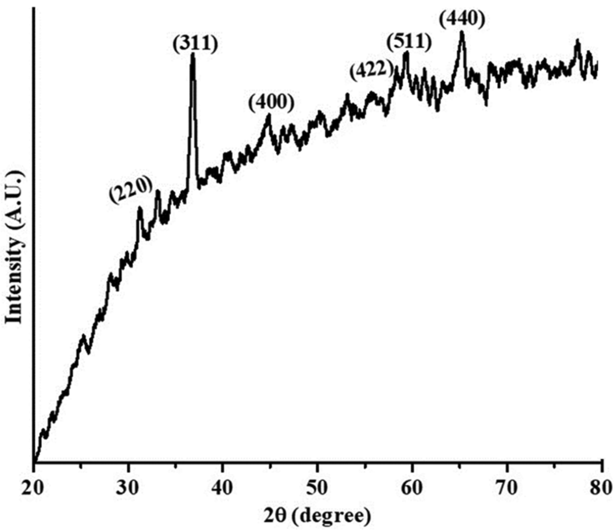

Fig 2 — XRD spectrum of Co_3O_4 prepared at 350°Cfor 5hrs

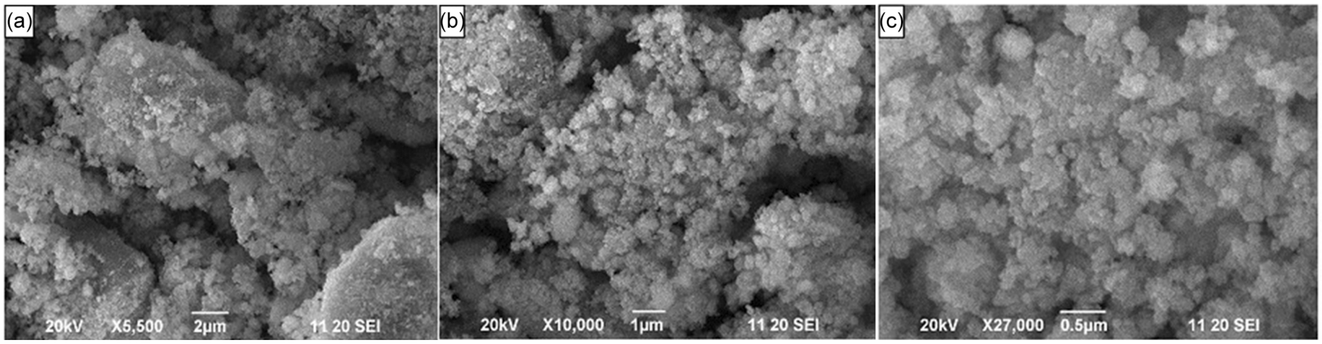

Fig 3 — SEMmicrograph of Co_3O_4 oxide at different magnifications(a) 5500X (b) 10000X (c) 27000X

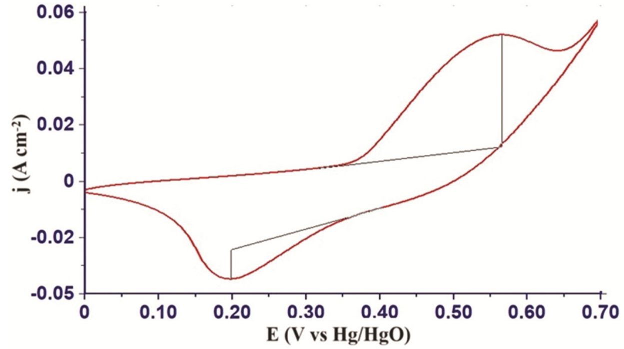

Fig 4 — Cyclic voltammetric curve of Ni/Co_3O_4electrode at scan rate of 20 mV s^{-1} in 1M KOH at 25°C.

comparatively less than that obtained by Gopinath *et al*[29].

SEM analysis

In order to know the surface morphology of the oxides, the scanning electron micrographs of Co_3O_4 oxide powder sintered at 350°C for 5 hours were taken at different modifications. The SEM micrographs of oxide powder at different magnifications (5500X, 10000X, and 27000X) were taken and shown in Fig 3. As seen in the SEM image, the oxide nanoparticles lies in agglomerated form with regular shape and particle size ranging between 200 to 300 nm.

Cyclic voltammetry

Cyclic voltammograms of fabricated electrode (Ni/Co_3O_4) were recorded at the scan rates of 20 mV sec^{-1} between potential regions 0 and 0.7 V *vs* Hg/HgO in 1M KOH at 25°C (Fig 4). From the CV curve, it is clear that a redox couple forms across oxide/KOH interface just onset of oxygen evolution reaction. The voltammogram exhibited pseudocapacitive in nature with anodic peak potential (E_{pa}= 566mV), cathodic peak potential (E_{pc}= 198 mV), ΔE_p= 368 mV and formal redox potential, E^o = 382 mV. These peak potential values correspod to redox reaction Co (IV) + e^- ↔ Co (III)[30]. Voltammogram also indicated that the ratio of anodic peak current to cathodic peak current is greater than unity. This shows that th≠e redox process is irriversible.

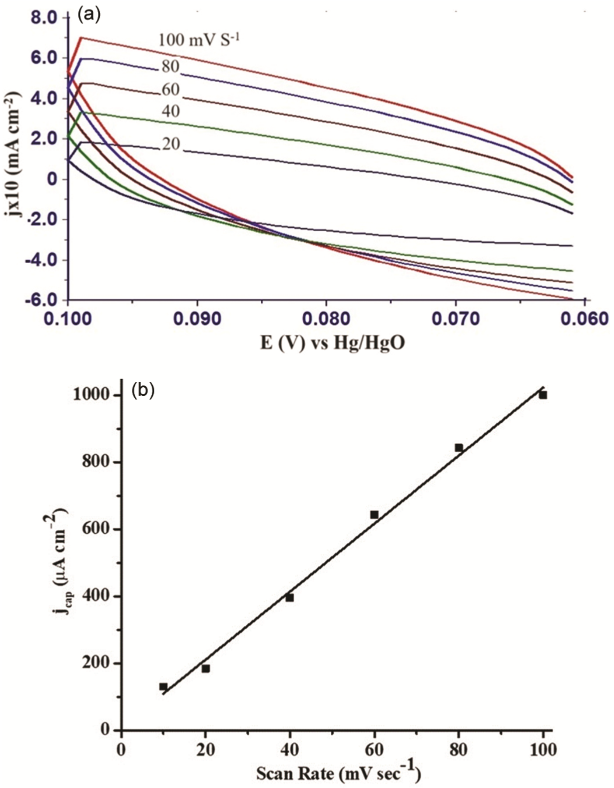

Fig 5(a) — CV curves of Ni/Co_3O_4 electrode at different scan rates in 1 M KOH at 25°C; (b) Plot of charging current density *vs*. scan rate for Ni/Co_3O_4 electrode

Roughness factor (R_F)

For the determination of the oxide roughness factor (R_F) of cobaltite oxide, cyclic voltammograms were recorded at different scan rates (10, 20, 40, 60, 80, and 100 mV s^{-1}) in 1 M KOH solution at 25°C between potential regions 0.06 and 0.1V where there is no interference of Faradic reactions (Fig 5(a)). The double layer capacitance(C_{dl}) was measured from the

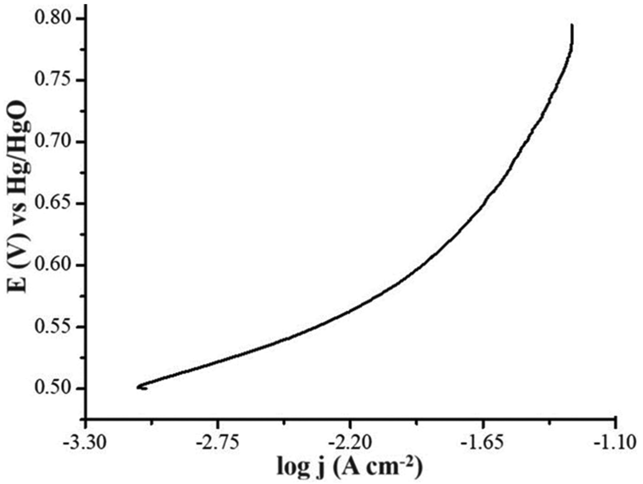

Fig 6 — Tafel polarization curve of Ni/Co_3O_4 electrode at 25°C in 1M KOH

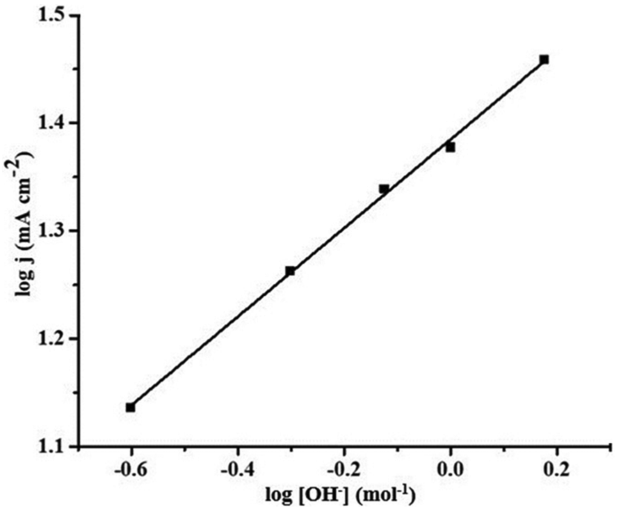

Fig 7 — Plot of log j (at E = 0.75V) *vs* log $[OH^-]$ for Ni/Co_3O_4 electrode at 25°C

slope of the straight line curve log j *vs* scan rate and the calculated value of C_{dl} was 1014.7μF for the cobaltite (Fig. 5(b)). The roughness factor for the oxide electrode was calculated from the C_{dl} values by assuming that the C_{dl} of the smooth oxide surface is 60μF[30]. The calculated value of R_F was observed to be ~ 169.

Electrocatalytic activity

Electrocatalytic activities for oxygen evolution on fabricated cobaltite electrodes were measured from the Tafel polarization curve recorded at0.5 mV s^{-1} scan rate in 1M KOH at 25°C, as shown in Fig 6. The polarization curve of Ni/Co_3O_4 electrode showed the Tafel slope value of 73 mV dec^{-1} in lower potential region and current density of 56 mA at 0.7 V *vs* Hg/HgO/1M KOH. From the polarization curve of electrodes tested for their OER electrocatalytic activity, it is clear that investigated oxide electrode showed comparitevely more electrocatalytic activity for OER with current density stand point than the same oxide prepared by other methods such as spray pyrolysis Co_3O_4 film coated on CdO glass and Ti[31,32], and sol-gel method Co_3O_4 film on graphide polyisobutylene[33].

Order of reaction

For the determination of the order of OER, the Tafel polarization curves were performed in various concentrations of KOH (*viz*., 0.25, 0.5, 0.75, 1.0, and 1.5 M) and the ionic strength of medium (μ= 1.5) was kept constant with the use of aninert electrolyte as KNO_3 at 25°C. The order of reaction was estimated from the slope of log j*vs* log [OH^-] plot at constant potential (0.75V) (Fig 7). The order of reaction for the oxide electrode was found to be approximately unity (~1) which indicated that the electrochemical formation of oxygen on the electrode/solution interface follows similar mechanism as found by Singh and co-workers[31].

Activation energy

The apparent electrochemical activation energy at reversible potential $(\Delta H_C^{O\neq})$, standard electrochemical activation energy $(\Delta H_{el}^{o\neq})$ at applied potential, and standard entropy of reaction $(\Delta S_{el}^{o\neq})$ are determined from the Tafel plot of oxide electrode recorded at different temperatures in 1 M KOH. The value of$(\Delta H_{el}^{o\neq})$was calculated from the slope of the Arrhenius plot (log j *vs*. 1/T) where j and T are the apparent current density and temperature in absolute degree and found to be ~ 35 kJ mol^{-1}. The calculated values of $(\Delta H_{el}^{o\neq})$, and $(\Delta S_{el}^{o\neq})$ are ~94 kJ mol^{-1} and –259 J $deg^{-1}mol^{-1}$, respectively. The standard entropy of reaction with negative value suggest the occurrence of adsorption phenomenon in OER on the surface of electrode.

Conclusions

The present investigation includes the preparation of cobaltite by sol-gel route using span–60 as a precursor. The formation of the spinel phase of oxide was established by the IR, XRD, and SEM analyses. The Span–60 sol-gel method could be useful for the cheaper production of oxide electrocatalysts for oxygen evolution reaction in alkaline medium. Cobaltite prepared by this method has higher electrocatalytic activity than those oxides obtained by the other conventional high-temperature methods and the present study recommends them as good candidates for electrocatalytic applications and energy storage devices.

Acknowledgments

One of the authors B. Lal is grateful to the UPCST for the financial support through a research grant (CST/CHEM/D-1120 ID-1167) and also to Prof. D.K. Das, Head of the Department of Chemistry, GLA University Mathura for providing the required research facilities.

References

1 Lewis N S & Nocera D G, *Proc Natl Acad Sci* USA, 103 (2006) 15729.

2 Li W Y, Xu L N & Chen J, *Adv Funct Mater*, 15 (2005) 851.

3 Wu R J, Wu J G, Yu M R, Tsai T K &Yeh C T, *Sens. Actu B Chem*, 131 (2008) 306.

4 Davies T E, García T, Solsona B, & Taylor S H, *Chem Commun*, 32 (2006) 3417.

5 Mate V R, Shirai M, & Rode C V, *Catal Commun*, 33 (2013) 66.

6 Lou X W, Deng D, Lee J Y, Feng J & Archer L A, *Adv Mater*, 20 (2008) 258.

7 Chou S L, Wang J Z, Liu H K & Dou S X, *J Power Sources* 182 (2008) 359.

8 Li Y, Tan B & Wu Y, *Nano Lett*, 8 (2008) 265.

9 Makhlouf S A, *J Magn Magn Mater*, 246 (2002) 184.

10 Lou X, Han J, Chu W, Wang X, & Cheng Q, *Mater. Sci. Eng. B*, 137 (2007) 268.

11 Warang T, Patel N, Santini A, Bazzanella N, Kale A, & Miotello A, *Appl Catal A Gen*, (2012) 21. (https://doi.org/10.1016/j.apcata.2012.02.037).

12 Sun L, Li H, Ren L & Hu C, *Solid State Sci*, 11 (2009) 108.

13 Chen Y, Zhang Y & Fu S, *Mater Lett*, 61 (2007) 701.

14 Lai T L, Lai Y L, Lee C C, Shu Y Y & Wang C B, *Catal Today*, 131 (2008) 105.

15 Li L, Chu Y, Liu Y, Song J, Wang D & Du X, *Mater Lett*, 62 (2008) 1507.

16 Du J, Chai L, Wang G, Li K & Qian Y, *J Chem*, 61 (2008) 153.

17 Li Y, Zhao J, Dan Y, Ma D, Zhao Y, Hou S & Wang Z, *Chem Engg*, 166 (2011) 428.

18 Sun H, Ahmad M & Zhu J, *Electrochim Acta*, 89 (2013) 199.

19 Ren M, Yuan S, Su L & Zhou Z, *Solid State Sci*, 14 (2012) 451.

20 Mc Crory C C, Jung S, Ferrer I M, Chatman S M, Peters J C & Jaramillo T F, *J Am Chem Soc*, 137 (2015) 4347.

21 Burke M S, Zou S, Enman L J, Kellon J E, Gabor C A, Pledger E & Boettcher S W, *J Phys Chem Lett* ,6 (2015) 3737.

22 Dong Y, He K, Yin L & Zhang A, *Nanotechnology,* 18 (2007) 435602.

23 Alvarado S R, Guo Y, Ruberu T P, Bakac A & Vela J, *J Phys Chem* C, 116 (2012), 10382.

24 Bergmann A, Martinez-Moreno E, Teschner D, Chernev P, Gliech M, de Araujo J F, Reier T, Dau H &Strasser P, *Nat Commun* 6 (2015) 8625.

25 Esswein A J, McMurdo M J, Ross P N, Bell A T & Tilley T D, *J PhysChem C*, 113 (2009) 15068.

26 Hull C M, Koza J A & Switzer J A, *J Mater Res*, 31 (2016) 3324.

27 Lal B, Singh N K, Samuel S & Singh R N, *J New Mat Eletrochem System*, 2 (1999) 59.

28 Abdallah A M &Awad R, *J Supercond Nov Magn,* 33 (2020)1395.

29 Gopinath S, Sivakumar K, Karthikeyan B, Ragupathi C & Sundaram R, *Physica E Low Dimens Syst Nanostruct,* 81 (2016) 66.

30 Lal B, Singh R N, & Singh N K, *J New Mat Eletrochem System*, 21 (2018) 163.

31 Singh R N, Hamdani M, Koenig J F, Poillerat G, Gautier J L & Chartier P, *J Appl Electrochim*, 20 (1990) 442.

32 Singh R N, Koenig J F, Poillerat G &Chartier P, *J ElectrochemSoc*, 137 (1990) 1408.

33 Baydi M, Poillerat G, Rehspringer J L, Gautier J L, Koenig J F & Chartier P, *J Solid State Chem*, 109 (1994) 281.